AIAA JOURNAL
Vol. 33, No. 3, March 1995

Analysis of Beam Contact Problems via Optimal Control Theory

Dewey H. Hodges*
Georgia Institute of Technology, Atlanta, Georgia 30332-0150
and
Robert R. Bless†
Lockheed Engineering and Science Company, Hampton, Virginia 23666

A class of large-deflection contact problems for beams is treated within the framework of optimal control theory, using an automated software system developed for variational optimization (e.g., trajectory optimization). Analysis of both Euler–Bernoulli and Timoshenko-type models is presented. Essentially exact numerical solutions are obtained by shooting, and the accuracy of a very efficient mixed finite element approach on which the automated software is based is demonstrated. Advantages of posing the problem within the optimal control framework are discussed. These include 1) being able to establish from the Euler–Bernoulli equations the existence of a physically inappropriate touch-point solution and 2) the ease by which an integral of the governing equations can be found to independently check the accuracy of a numerical solution.

Introduction

THE buckling of a beam was set up as an optimal control problem by Bryson and Ho.[1] The running length coordinate is the independent variable analogous to time, the length of the beam to the final time, the deflection and section rotation to the states, the total energy (strain energy and potential of the applied load) to the performance index, the strain measures to the controls, and the section force and moment to the costates.

There are some distinct advantages to posing contact problems within the optimal control framework. First, optimal control theory is now in a highly developed form, able to incorporate state and control inequality constraints rather naturally, and provides insight into the jump conditions which result from these constraints. Thus, it is hoped that this paper will shed light on certain anomalous results in the solution of elementary contact problems for beams. Second, there are now many software tools for solving a wide variety of optimization and optimal control problems.[2–5] VTOTS is such a tool that solves optimal control problems via temporal finite elements[6]; the finite element formulation associated with VTOTS is described in detail in Refs. 7–9. This package allows for the analyst to simply enter the performance index and specify the states, the control variables, and the relationships between them. At this point the software system generates an appropriate finite element program, compiles it, executes it, and outputs the solution. If the finite element results are not sufficiently accurate, the analyst can either refine the mesh or use the results as initial guesses for a shooting algorithm to obtain an essentially exact solution.

There is a large body of literature on the finite element approach to contact problems for beams. For example, Ref. 10 develops a finite element approach to the contact problem based on the slack-variable approach. The finite element results exhibit reasonably good agreement with solutions obtained by other means, although there is considerable oscillation in the finite element results. Reference 11 develops a finite element approach to the contact problem based on the displacement method. This approach suggests that adjustment of the location of the boundary node between areas of contact and noncontact leads to improved convergence. However, the work notes the difficulty in distinguishing touch-point results from those which just have a small contact area. Reference 12 develops a mixed finite element approach, pointing out some advantages of mixed methods over displacement methods for this problem. Reference 13 develops an error estimation technique for the finite element solution of beam contact problems. Reference 14 extends the displacement finite element approach for beam contact problems to the large-displacement case.

In this paper the problem of a laterally loaded elastic beam which comes in contact with a smooth, flat surface is considered. This class of problems can be treated analytically under certain circumstances, such as when the problem is restricted to small deformation. For example, in Ref. 15 an analysis of a loaded Euler–Bernoulli beam resting on a table, but with one end extending beyond the table edge, is presented. The weight of the overhanging portion causes some of the part on the table to be raised up, whereas the rest lies flat on the table. The analysis reveals that the shear force must jump, from zero in the region of contact with the table, to a nonzero value dependent on the distributed load in the region which is not in contact. The presence of such a jump is disturbing on physical grounds. However, more advanced analytical treatments[16,17] show that with transverse shear deformation, a far more realistic description of the physical problem is obtained. (Addition of transverse normal strain provides further improvement,[18] but will not be considered herein.)

Approximate solution of contact problems can be approached through special-purpose finite element programs. However, here we will take advantage of the analogy with optimal control problems to solve problems of beam contact with a general-purpose optimal control software system.[6] The beam is homogeneous and isotropic and undergoes planar deformation. The analysis is based on the geometrically exact strain-displacement relations of Reissner[19] and the usual constitutive relations of Timoshenko beams. The finite element method of Refs. 7–9 uses piecewise constant trial functions for all variables, piecewise constant test functions for the control (strains for this problem), and piecewise linear functions for the states (displacements) and co-states (stress resultants). This leads to very sparse coefficient matrices and closed-form, exact quadrature over the element length.

Therefore, there are four objectives of this paper: 1) to call attention to the utility of the optimal control analogy for the beam, 2) to show that the solution of optimal control problems with state inequality constraints provides a suitable framework for solving contact problems, 3) to illustrate an application of a mixed finite element method in the presence of unilateral constraints, and 4) to use this framework to explore some additional reasons for the known importance of shear deformation for this class of problem.

Statement of the Problem

We consider a simply supported beam of length ℓ, loaded with a uniform distributed load of magnitude q, and suspended at a height $h\ell$ above a rigid, flat, smooth support, as shown in Fig. 1. The

Received May 13, 1994; revision received Nov. 21, 1994; accepted for publication Nov. 23, 1994.

*Professor, School of Aerospace Engineering. Fellow AIAA.
†Senior Engineer, 144 Research Drive. Member AIAA.

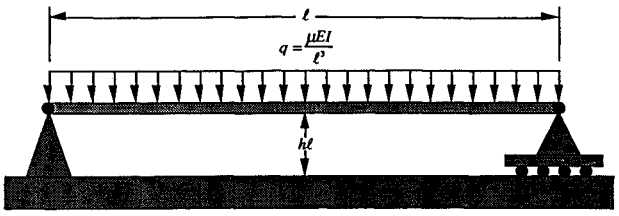

Fig. 1 Schematic of loaded beam.

deformation of the beam is described in terms of horizontal displacement of points on the reference line ℓu (positive to the right), vertical displacement of points on the reference line ℓv (positive upward), and cross-sectional rotation θ (positive counterclockwise). (The reference line is taken as the axis of cross-sectional centroids.) The quantities $u(x)$, $v(x)$, and $\theta(x)$ play the role of states in the optimal control formulation, where ℓx is the running length coordinate which is analogous to time. Note that $0 \leq x \leq 1$.

The strain measures[19] are taken as

$$\begin{aligned} \epsilon &= (1+u')\cos\theta + v'\sin\theta - 1 \\ \gamma &= -(1+u')\sin\theta + v'\cos\theta \\ \kappa &= \theta' \end{aligned} \tag{1}$$

where $()' = \mathrm{d}()/\mathrm{d}x$, ϵ is the stretching of the reference line, γ is the transverse shear strain measure, and κ is the bending strain measure. When the strain energy per unit length U is expressed in terms of these strain measures, the derivatives of U with respect to ϵ, γ, and κ are the component of the section force normal to the cross-sectional plane, the component of the section force parallel to the cross-sectional plane (the transverse shearing force), and the bending moment, respectively. These relations hold even for large deflections. The strain measures ϵ, γ, and κ play the role of control variables in the optimal control formulation.

The strain-displacement equations, Eqs. (1), are now inverted to obtain the "state" equations

$$\begin{aligned} u' &= (1+\epsilon)\cos\theta - \gamma\sin\theta - 1 \\ v' &= (1+\epsilon)\sin\theta + \gamma\cos\theta \\ \theta' &= \kappa \end{aligned} \tag{2}$$

which will be adjoined to the performance index with Lagrange multiplier functions denoted by λ_u, λ_v, and λ_θ, respectively. The state constraint is

$$S = -(v+h) \leq 0 \qquad \forall x \tag{3}$$

Since S is independent of control variables, it is differentiated with respect to x until a control variable appears explicitly.[1] That derivative is then adjoined to the performance index with the Lagrange multiplier function η.

In light of the freedom of the right end to translate left and right, the stretching of the beam reference line can be neglected. Thus, $\epsilon = 0$ and, in addition to h, the problem is governed by the dimensionless parameters

$$\begin{aligned} g &= GK\ell^2/EI \\ \mu &= q\ell^3/EI \end{aligned} \tag{4}$$

where EI is the bending rigidity and GK the transverse shear rigidity. It should be noted that κ plays the role of the dimensionless bending moment in the beam, given by the dimensional bending moment divided by EI/ℓ. Similarly, the dimensionless shear force is denoted by V and is given by the dimensional shear force divided by EI/ℓ^2.

Timoshenko Theory

The resulting nonlinear theory is referred to herein as Timoshenko beam theory. The performance index is the total strain and potential energy and is given by

$$J = \frac{1}{2}\int_0^1 (\kappa^2 + g\gamma^2 + 2\mu v)\,\mathrm{d}x \tag{5}$$

The state equations reduce to

$$\begin{aligned} u' &= \cos\theta - \gamma\sin\theta - 1 \\ v' &= \sin\theta + \gamma\cos\theta \\ \theta' &= \kappa \end{aligned} \tag{6}$$

where κ and γ are now the only control variables. The state inequality constraint S does not depend explicitly on the controls. Thus, it is differentiated once, yielding $S' = -v' = -(\sin\theta + \gamma\cos\theta)$, which is an explicit function of γ. This makes it a first-order constraint which almost always exhibits a boundary-arc solution. The Hamiltonian is, therefore, given by

$$\mathcal{H} = \tfrac{1}{2}(\kappa^2 + g\gamma^2 + 2\mu v) - \eta v' + \lambda_u u' + \lambda_v v' + \lambda_\theta \theta' \tag{7}$$

where η is nonnegative when the constraint is active (i.e., when the beam is in contact with the surface) and zero otherwise. The costate equations are

$$\begin{aligned} \lambda_u' &= -\frac{\partial \mathcal{H}}{\partial u} = 0 \\ \lambda_v' &= -\frac{\partial \mathcal{H}}{\partial v} = -\mu \\ \lambda_\theta' &= -\frac{\partial \mathcal{H}}{\partial \theta} = \lambda_u(\sin\theta + \gamma\cos\theta) - (\lambda_v - \eta)(\cos\theta - \gamma\sin\theta) \end{aligned} \tag{8}$$

and the optimality conditions are

$$\frac{\partial \mathcal{H}}{\partial \gamma} = g\gamma - \lambda_u\sin\theta + (\lambda_v - \eta)\cos\theta = 0 \tag{9a}$$

$$\frac{\partial \mathcal{H}}{\partial \kappa} = \kappa + \lambda_\theta = 0 \tag{9b}$$

The boundary conditions are defined as

$$u(0) = 0 \tag{10a}$$

$$v(0) = 0 \tag{10b}$$

$$\lambda_\theta(0) = 0 \tag{10c}$$

$$v(1) = 0 \tag{10d}$$

$$\lambda_u(1) = 0 \tag{10e}$$

$$\lambda_\theta(1) = 0 \tag{10f}$$

and with the state constraint active, we add internal boundary conditions

$$\begin{aligned} v(x_1) + h &= 0 \\ \lambda_v(x_1^+) &= \lambda_v(x_1^-) - \nu \end{aligned} \tag{11}$$

where ν is an unknown constant and x_1 is the smallest value of x at which the beam touches the support.

In light of the differential equation and boundary condition governing λ_u, it is clear that $\lambda_u(x) = 0$ and may be identified as the horizontal component of the section force. Thus, the dimensionless shear force, which in this theory is most naturally given by

$$V = \frac{\partial U}{\partial \gamma} = g\gamma \tag{12}$$

can also be obtained from Eq. (9) as

$$V = -(\lambda_v - \eta)\cos\theta \tag{13}$$

When the constraint is not active, $\eta = 0$, and λ_v is identified as the vertical component of the section force (dimensionless). In any case, the continuity of the control variable γ assures us of a continuous shear force distribution for constant g. Finally, note from Eq. (9b) that $\lambda_\theta = -\kappa$ which is the negative of the dimensionless bending moment in the beam.

Euler–Bernoulli Theory

For the Euler–Bernoulli beam theory, in addition to $\epsilon = 0$, we take $\gamma = 0$. The total energy (strain and potential) reduces to

$$J = \int_0^1 \left(\frac{\kappa^2}{2} + \mu v\right) dx \tag{14}$$

and the state equations to

$$\begin{aligned} u' &= \cos\theta - 1 \\ v' &= \sin\theta \\ \theta' &= \kappa \end{aligned} \tag{15}$$

where κ is now the only control variable. Now $S' = -v' = -\sin\theta$ is independent of κ. Another differentiation yields $S'' = -\kappa\cos\theta$. Note that this is now a second-order constraint which allows for either a touch-point or a boundary-arc solution. The Hamiltonian is defined as

$$\mathcal{H} = \tfrac{1}{2}\kappa^2 + \mu v - \eta\kappa\cos\theta + \lambda_u u' + \lambda_v v' + \lambda_\theta \theta' \tag{16}$$

where, again, η is nonnegative when the constraint is active and zero otherwise. The costate equations are

$$\lambda_u' = -\frac{\partial \mathcal{H}}{\partial u} = 0 \tag{17a}$$

$$\lambda_v' = -\frac{\partial \mathcal{H}}{\partial v} = -\mu \tag{17b}$$

$$\lambda_\theta' = -\frac{\partial \mathcal{H}}{\partial \theta} = \lambda_u \sin\theta - \lambda_v \cos\theta - \eta\kappa\sin\theta \tag{17c}$$

and the optimality condition is

$$\frac{\partial \mathcal{H}}{\partial \kappa} = \kappa + \lambda_\theta - \eta\cos\theta = 0 \tag{18}$$

The boundary conditions are given in Eq. (10), and with the state constraint active we add the internal boundary conditions

$$\begin{aligned} v(x_1) + h &= 0 \\ v'(x_1) = \sin\theta(x_1) &= 0 \\ \lambda_v(x_1^+) &= \lambda_v(x_1^-) - \nu_1 \\ \lambda_\theta(x_1^+) &= \lambda_\theta(x_1^-) - \nu_2\cos\theta \end{aligned} \tag{19}$$

where ν_1 and ν_2 are unknown constants. Again, from Eqs. (10e) and (17a), we can identify $\lambda_u(x) = 0$.

In accordance with Euler–Bernoulli beam theory, the shear force is the negative of the derivative of the bending moment so that

$$V = -\kappa' \tag{20}$$

which, according to Eq. (18), is given by

$$V = (\lambda_\theta - \eta\cos\theta)' \tag{21}$$

Substituting Eq. (17c), one obtains

$$V = -(\lambda_v + \eta')\cos\theta \tag{22}$$

When the constraint is inactive, $\eta = \eta' = 0$, and the result agrees with Eq. (13). In other words, since the differential equation for λ_v is identical for both cases, then the same value for the shear force is obtained for both the Timoshenko and Euler–Bernoulli beam theories when the constraint is inactive. However, when the constraint is active, $S'' = -\kappa\cos\theta = 0$, which leads to $\kappa = 0$ so that $V = 0$. Thus, in the Euler–Bernoulli case it is clear that V is not continuous, which is physically unrealistic. In this case there is no equation analogous to Eq. (12). Thus, the shear force is purely reactive, meaning that one cannot solve for it in terms of controls (i.e., strain measures) only.

In addition to the a priori prediction of the existence of boundary arcs or touch points for the two beam theories and the physical significance of the costates being identified as sectional forces and moments, optimal control theory offers another advantage. For both the Timoshenko and Euler–Bernoulli beam theories, the Hamiltonian $\mathcal{H}$ is a first integral and must be a constant over the entire beam length. For example, in the Euler–Bernoulli case with the constraint inactive, the constancy of the Hamiltonian reveals that

$$(\kappa^2/2) - \mu v + V\tan\theta = (V\tan\theta)|_{x=0} \tag{23}$$

Recognizing $V\tan\theta$ as the axial force (tangential to the deformed beam reference line), this is an extension of the first integral found by the Kirchhoff analogy[20]; it allows for a rigorous check of any numerical solution.

Results

The given optimal control problems were solved using the VTOTS software system,[6] which is based on mixed finite elements in the time domain[7]; essentially exact shooting results were subsequently obtained using the finite element results as initial guesses. The term mixed in the context of the beam problem means that unknowns include quantities other than displacement, such as the strain measures and the section force and moment. Some of the results obtained are given in Figs. 2–14. The value of g is fixed at 2500 whereas μ is varied from 0 to 200.

In Fig. 2, the maximum displacement $v|_{x=0.5}$ and maximum section rotation $\theta|_{x=0}$ vs μ with the constraint inactive are shown for the preceding nonlinear theories as well as for a linear version of the Euler–Bernoulli theory. It is clear that the nonlinear theory is necessary for the magnitude of the loads considered herein. However, as expected, very little difference is observed between the Timoshenko theory and nonlinear Euler–Bernoulli theory. No further linear results will be shown here.

In Figs. 3–7, results are presented for $h = 0.2$ and $\mu = 150$. The states (u, v, and θ) predicted by the two theories agree quite well, as shown in Fig. 3. It is observed from Fig. 4 that values of λ_v from the two theories agree well in the region where the constraint is inactive. Moreover, the values of λ_v from the two theories have the same qualitative behavior when the constraint is active; however, the predicted jump in this costate, due to the constraint, occurs at different places on the beam for the two theories. (The position and length of portion of the beam in contact with the surface will be examined subsequently.) Figure 5 shows that values of λ_θ predicted by the two theories agree well in the region where the constraint is

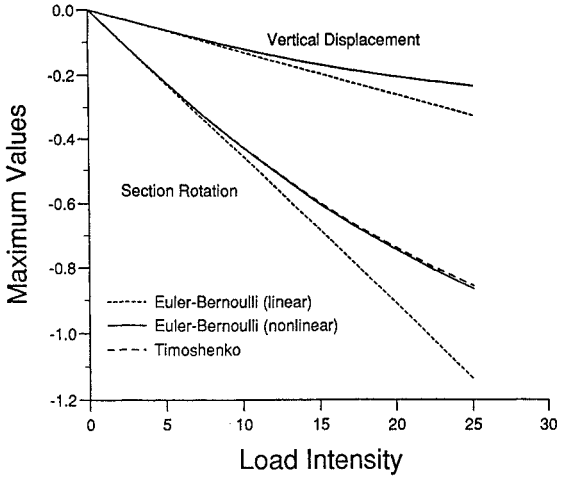

Fig. 2 Maximum displacement $v|_{x=0.5}$ and maximum section rotation $\theta|_{x=0}$ vs load intensity μ from both nonlinear theories and a linear Euler–Bernoulli theory.

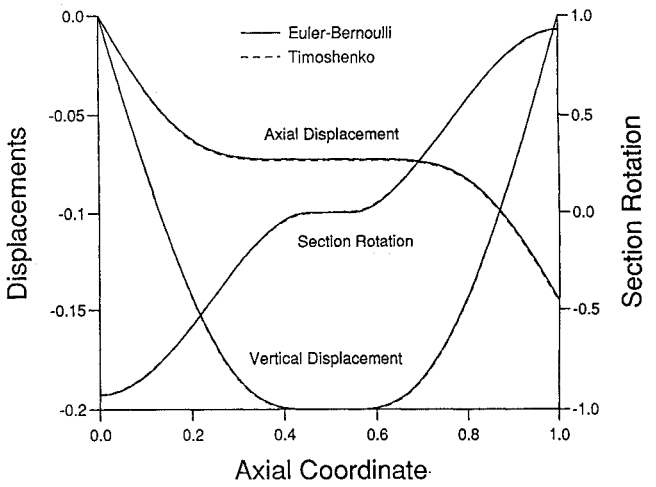

Fig. 3 Horizontal displacement u, vertical displacement v, and section rotation θ vs axial coordinate x from both nonlinear theories, $\mu = 150$ and $h = 0.2$.

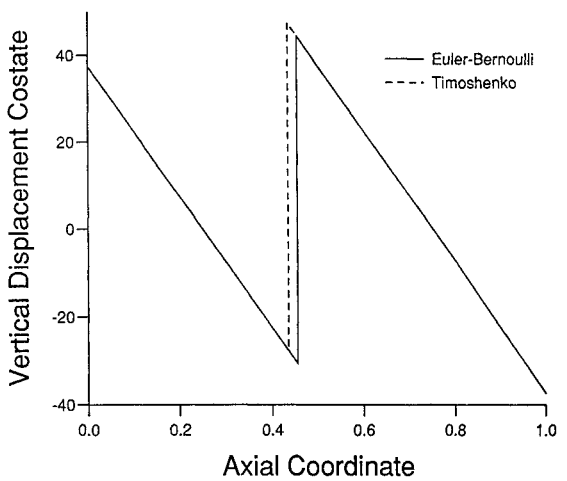

Fig. 4 Vertical displacement costate λ_v vs axial coordinate x from both nonlinear theories, $\mu = 150$ and $h = 0.2$.

inactive, but when the constraint is active there are some qualitative differences. It should be noted, however, that λ_θ for the Timoshenko theory has a different meaning from λ_θ of the Euler–Bernoulli theory. The optimality condition in the Timoshenko case, Eq. (9), reveals that $\lambda_\theta = -\kappa$. However, according to Eq. (18) this is only true in the Euler–Bernoulli case for points of the beam where the constraint is inactive (i.e., where $\eta = 0$).

One must compare quantities whose physical meaning is the same between the two theories to conclude anything. The bending moment κ is such a quantity. It is clear from Fig. 6 that the predicted κ is qualitatively different for the two theories when the constraint is active (note that κ is constrained to be zero for the Euler–Bernoulli theory). In Fig. 7 another physically meaningful quantity, the shear force V, is shown. When the constraint is inactive, the two theories agree quite well, as expected for slender beams. However, two things need to be observed. 1) The predicted length over which the constraint is active is quite different for the two theories, the Euler–Bernoulli theory predicting a much smaller contact length for this loading. 2) The predicted behavior of V is qualitatively different for the two theories. The Euler–Bernoulli result for V behaves similarly to that of the elementary example of Ref. 15 with a physically unrealistic jump. (This is reflecting a concentrated load—which appears to come out of nowhere!) On the other hand, the Timoshenko result is more realistic physically. Note, however, that it predicts a jump in the resultant load between the constrained and unconstrained regions, reflected in the discontinuity of the slope of V. A higher order beam theory can alleviate this[17] with rather modest quantitative changes in the remaining results.

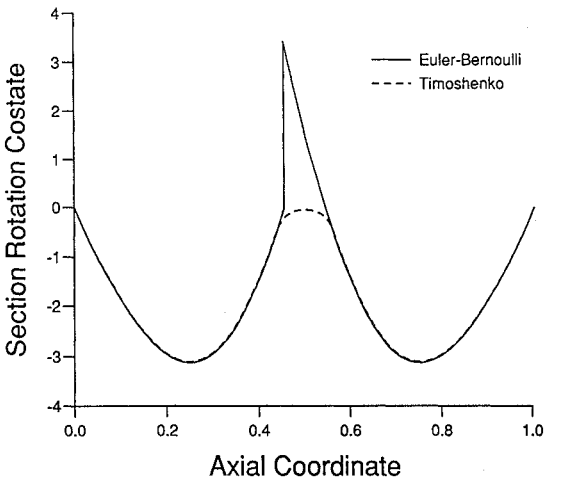

Fig. 5 Section rotation costate λ_θ vs axial coordinate x from both nonlinear theories, $\mu = 150$ and $h = 0.2$.

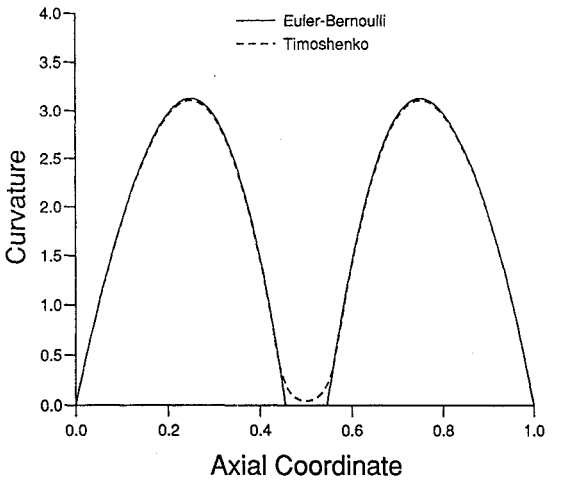

Fig. 6 Curvature κ (same as dimensionless bending moment) vs axial coordinate x from both nonlinear theories, $\mu = 150$ and $h = 0.2$.

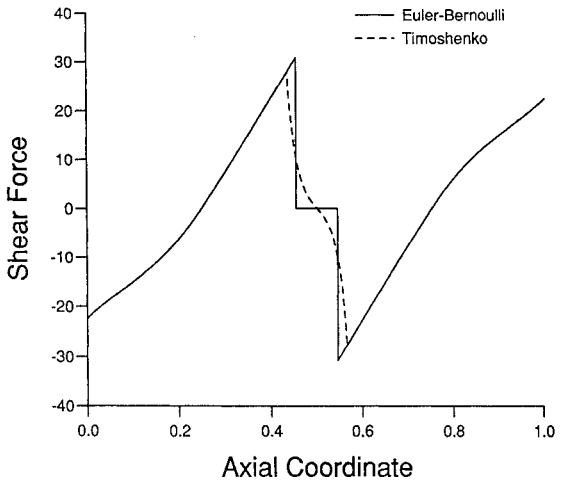

Fig. 7 Shear force V vs axial coordinate x from both nonlinear theories, $\mu = 150$ and $h = 0.2$.

Figure 8 shows the contact length as a function of μ. Notice the qualitative difference in the two solutions. The Euler–Bernoulli solution exhibits touch-point behavior consistent with second-order constraints, but the Timoshenko solution shows only boundary-arc behavior. The beam comes in contact with the surface in the two theories for nearly the same loading, as expected; but the Euler–Bernoulli touch-point solution shows (unrealistically) that the beam stays in contact at a single point until the load becomes nearly five

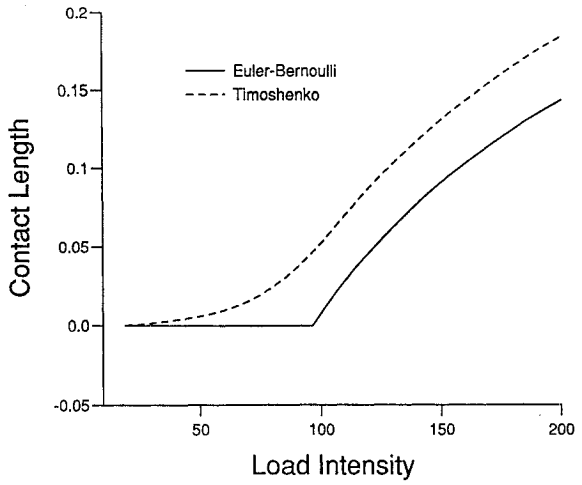

Fig. 8 Contact length vs load intensity μ for $h = 0.2$.

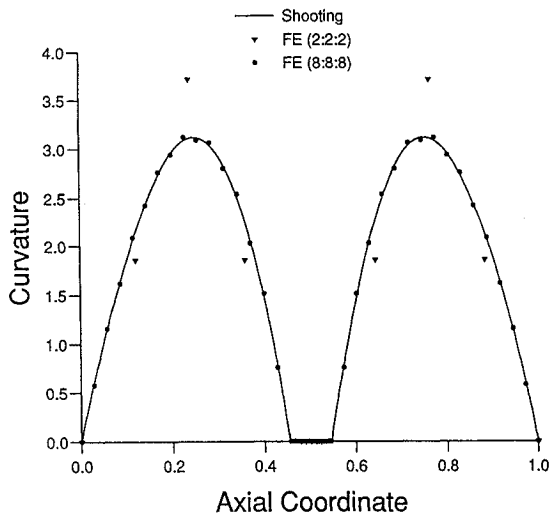

Fig. 9 Curvature κ vs axial coordinate x from Euler–Bernoulli theory: shooting (solid line), two finite elements per phase (▼), eight finite elements per phase (•), $\mu = 150$ and $h = 0.2$.

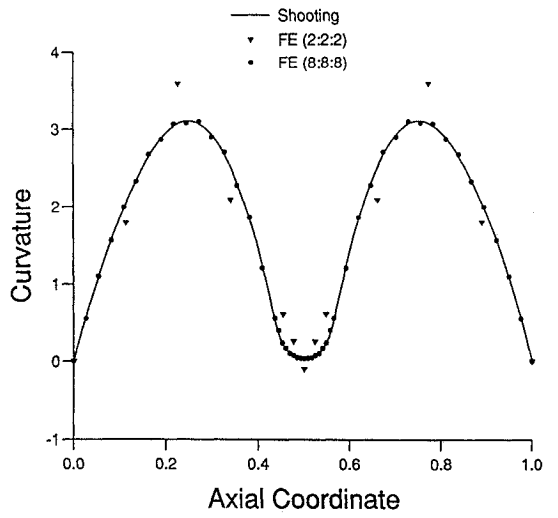

Fig. 10 Curvature κ vs axial coordinate x from Timoshenko theory: shooting (solid line), two finite elements per phase (▼), eight finite elements per phase (•), $\mu = 150$ and $h = 0.2$.

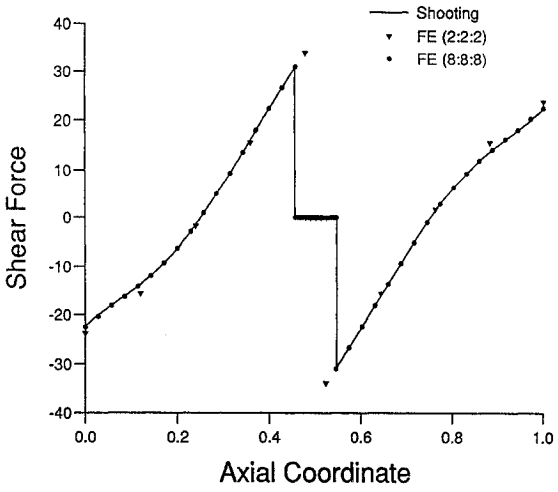

Fig. 11 Shear force V vs axial coordinate x from Euler–Bernoulli theory: shooting (solid line), two finite elements per phase (▼), eight finite elements per phase (•), $\mu = 150$ and $h = 0.2$.

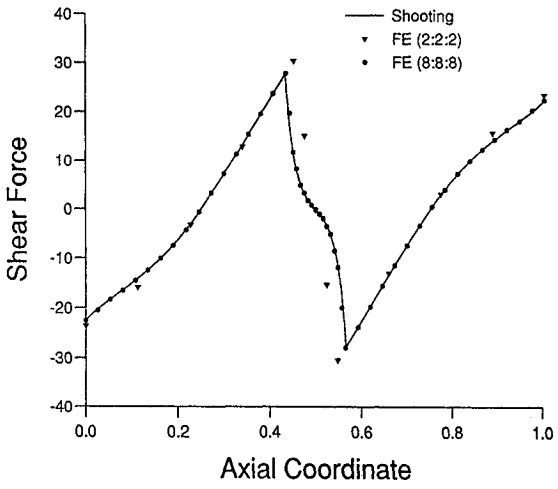

Fig. 12 Shear force V vs axial coordinate x from Timoshenko theory: shooting (solid line), two finite elements per phase (▼), eight finite elements per phase (•), $\mu = 150$ and $h = 0.2$.

times as large as the initial contact load (linear theory predicts exactly five)! Then, as the load is further increased the contact length begins to grow with load. On the other hand, the Timoshenko result shows a monotonic growth of contact length with load right from the point of first contact, again a more realistic result.

Figures 9–14 demonstrate the accuracy of the finite element method used to generate guesses for a shooting method. In Figs. 9–12, $h = 0.2$ and $\mu = 150$. The solid line is the shooting result, and two finite element cases are shown, one with two elements in each constrained and unconstrained section of the beam and one with eight elements per section. Figures 9 and 10 show the curvature from the Euler–Bernoulli and Timoshenko theories, respectively, vs finite element results; Figs. 11 and 12 show the shear force. It can be observed that the two-element case only very roughly approximates the solution; however, the eight-element case approximates the solution very reasonably. It is a simple matter to increase the number of elements even more if required.

Figure 13 shows the relative error of the contact length for $h = 0.2$ and $\mu = 150$ vs the total number of elements used to approximate the answer for the two theories. These results are nearly straight lines on a log-log scale, the slope of which is approximately -2. This means the method can be considered as a second-order method where the accuracy increases with the inverse of the square of the number of elements.

In Fig. 14 the pointwise relative error is shown for the unconstrained Timoshenko case with $\mu = 20$ and 16 finite elements. The relative error shown is for the Hamiltonian and the main states and controls. Except for γ, there is strong correlation between the

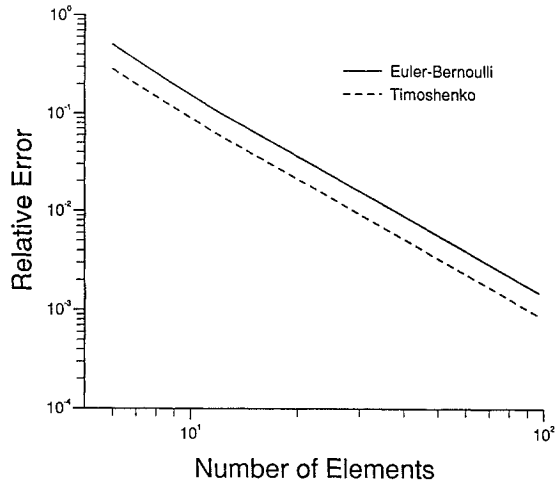

Fig. 13 Relative error of the contact length from the finite element solution vs number of elements, $\mu = 150$ and $h = 0.2$.

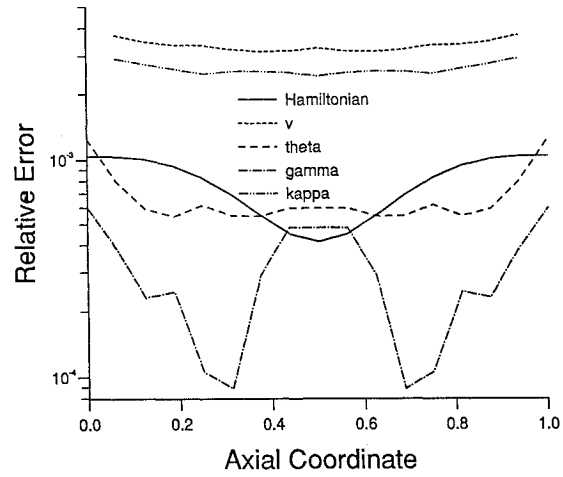

Fig. 14 Relative error of the Hamiltonian, states v and θ, and controls γ and κ from the finite element solution vs the axial coordinate, $\mu = 20$.

relative error of the Hamiltonian and that of the primary variables. In both cases, the largest errors are near the ends for this uniform mesh. One possible explanation for the Hamiltonian not picking up the error in γ is that the expression for the Hamiltonian can be shown to be equal to the Hamiltonian for the Euler–Bernoulli model minus $\frac{1}{2}V\gamma$, a term dominated by the other terms in the expression. In optimal control problems it is always possible to construct a Hamiltonian function that is exactly zero. Thus, it is suggested that departure of the Hamiltonian from its zero value is of potential use as an error indicator in finite element applications for adaptive p or h refinement of finite element solutions. The method presented herein provides one with a Hamiltonian function similar to functions referred to by Love[20] as energy integrals of deformation.

Closure

Large-deflection behavior of a laterally loaded uniform elastic beam in contact with a rigid, smooth, flat surface is analyzed within the framework of optimal control theory. Two different beam theories are used: one based on a Timoshenko model, including transverse shear deformation, and the other based on an Euler–Bernoulli model, excluding it. As is known, the Euler–Bernoulli model predicts that the shear force jumps at the boundary between the portions of the beam where the constraint is active and where it is inactive. Analysis of this problem within the optimal control framework reveals the source of this physically unreasonable behavior. In the Euler–Bernoulli theory, an expression for the shear force cannot be obtained in terms of controls (i.e., strain measures) only. Furthermore, the second-order state constraint implies the possibility of a touch-point solution—again, a physically unrealistic result in this context. On the other hand, optimal control theory guarantees a continuous shear force for the Timoshenko theory, since the transverse shear strain measure is a continuous control variable. Additionally, optimal control theory provides a first integral which may be used as an independent check of a numerical solution.

References

[1]Bryson, A. E., Jr., and Ho, Y.-C., *Applied Optimal Control*, Hemisphere, New York, 1975, p. 191.

[2]Gill, P. E., Murray, W., Saunders, M. A., and Wright, M. H., "User's Guide for NPSOL (Version 4.0): A FORTRAN Package for Nonlinear Programming," Systems Optimization Lab., Dept. of Operations Research, Stanford Univ., Stanford, CA.

[3]Oberle, H. J., and Grimm, W., "BNDSCO: A Program for the Numerical Solution of Optimal Control Problems," English Translation of DLR-Mitt. 85-05, Oberpfaffenhofen, Germany.

[4]Betts, J. T., and Huffman, W. P., "Trajectory Optimization on a Parallel Processor," *Journal of Guidance, Control, and Dynamics*, Vol. 14, No. 2, 1991, pp. 431–439.

[5]Hargraves, C. R., and Paris, S. W., "Direct Trajectory Optimization Using Nonlinear Programming and Collocation," *Journal of Guidance, Control, and Dynamics*, Vol. 10, No. 4, 1987, pp. 338–342.

[6]Bless, R. R., Queen, E. M., Cavanaugh, M. D., Wetzel, T. A., and Moerder, D. D., "Variational Trajectory Optimization Tool Set: Technical Description and User's Manual," NASA TM 4442, July 1993.

[7]Hodges, D. H., and Bless, R. R., "Weak Hamiltonian Finite Element Method for Optimal Control Problems," *Journal of Guidance, Control, and Dynamics*, Vol. 14, No. 1, 1991, pp. 148–156.

[8]Bless, R. R., and Hodges, D. H., "Finite Element Solution of Optimal Control Problems with State-Control Inequality Constraints," *Journal of Guidance, Control, and Dynamics*, Vol. 15, No. 4, 1992, pp. 1029–1032.

[9]Bless, R. R., Hodges, D. H., and Seywald, H., "A Finite Element Method for the Solution of State-Constrained Optimal Control Problems," *Journal of Guidance, Control, and Dynamics* (to be published).

[10]Hung, N. D., and de Saxcé, G., "Frictionless Contact of Elastic Bodies by Finite Element Method and Mathematical Programming Technique," *Computers and Structures*, Vol. 11, 1980, pp. 55–67.

[11]Westbrook, D. R., "Contact Problems for the Elastic Beam," *Computers and Structures*, Vol. 15, No. 4, 1982, pp. 473–479.

[12]Ostachowicz, W., "Mixed Finite Element Method for Contact Problems," *Computers and Structures*, Vol. 18, No. 5, 1984, pp. 937–945.

[13]Bermúdez, A., and Fernández, J., "Solving Unilateral Problems for Beams by Finite Element Methods," *Computer Methods in Applied Mechanics and Engineering*, Vol. 54, 1986, pp. 67–73.

[14]Lee, G. B., and Kwak, B. M., "Formulation and Implementation of Beam Contact Problems under Large Displacement by a Mathematical Programming," *Computers and Structures*, Vol. 31, No. 3, 1989, pp. 365–376.

[15]Crandall, S. H., Dahl, N. C., and Lardner, T. J., *An Introduction to the Mechanics of Solids*, McGraw-Hill, New York, 1978, Example 8.5, pp. 524–527.

[16]Essenburg, F., "On Surface Constraints in Plate Problems," *Journal of Applied Mechanics*, Vol. 29, No. 2, 1962, pp. 340–344.

[17]Essenburg, F., "On the Significance of the Inclusion of Transverse Normal Strain in Problems Involving Beams with Surface Constraints," *Journal of Applied Mechanics*, Vol. 42, No. 1, 1975, pp. 127–132.

[18]Naghdi, P. M., and Rubin, M. B., "On the Significance of Normal Cross-Sectional Extension in Beam Theory with Application to Contact Problems," *International Journal of Solids and Structures*, Vol. 25, No. 3, 1989, pp. 249–265.

[19]Reissner, E., "On One-Dimensional Finite-Strain Beam Theory: The Plane Problem," *Journal of Applied Mathematics and Physics (ZAMP)*, Vol. 23, 1972, pp. 795–804.

[20]Love, A. E. H., *A Treatise on the Mathematical Theory of Elasticity*, Dover, New York, 1944, Art. 260.